The Journal of Experimental Biology 209, 3587-3598
Published by The Company of Biologists 2006
doi:10.1242/jeb.02423

Odour-evoked responses to queen pheromone components and to plant odours using optical imaging in the antennal lobe of the honey bee drone *Apis mellifera* L.

Jean-Christophe Sandoz

Research Centre for Animal Cognition, UMR 5169, Université Paul Sabatier, 118, Route de Narbonne, 31062 Toulouse cedex 4, France

e-mail: sandoz@cict.fr

Accepted 3 July 2006

Summary

The primordial functional role of honey bee males (drones) is to mate with virgin queens, a behaviour relying heavily on the olfactory detection of queen pheromone. In the present work I studied olfactory processing in the drone antennal lobe (AL), the primary olfactory centre of the insect brain. In drones, the AL consists of about 103 ordinary glomeruli and four enlarged glomeruli, the macroglomeruli (MG). Two macroglomeruli (MG1 and MG2) and approximately 20 ordinary glomeruli occupy the anterior surface of the antennal lobe and are thus accessible to optical recordings. Calcium imaging was used to measure odour-evoked responses to queen pheromonal components and plant odours. MG2 responded specifically to the main component of the queen mandibular pheromone, 9-ODA. The secondary components HOB and HVA each triggered activity in one, but not the same, ordinary glomerulus. MG1 did not respond to any of the tested stimuli. Plant odours induced signals only in ordinary glomeruli in a combinatorial manner, as in workers. This study thus shows that the major queen pheromonal component is processed in the most voluminous macroglomerulus of the drone antennal lobe, and that plant odours, as well as some queen pheromonal components, are processed in ordinary glomeruli.

Key words: olfaction, insect, calcium imaging, antennal lobe, sex pheromone, sexual communication.

Introduction

In honey bees, as in most insect species, mating behaviour relies heavily on olfaction, as the queen produces a complex range of pheromonal components, some of which are attractive to males (Free, 1987). Queen pheromonal components also play a crucial social role, since they maintain the colony's cohesion, influencing both the physiology and the behaviour of worker bees (Free, 1987; Winston, 1987). Thus queen pheromonal components act both as a primer pheromone, inhibiting the ovarian development in workers, and as a releaser pheromone, attracting workers to form a retinue around the queen, stimulating social pheromone production by workers, controlling swarming, etc (Free, 1987; Winston, 1987). Two of the main components of the queen pheromone, produced in the mandibular glands, are 9-keto-2 (E)-decenoic acid (9-ODA) and 9-hydroxy-2 (E)-decenoic acid (9-HDA). The 9-ODA, in particular, was shown to be highly effective in male-attraction bioassays (Gary, 1962; Butler and Fairey, 1964). However, the two compounds 9-ODA and 9-HDA, both alone or blended, are less effective than a whole-queen extract in eliciting retinue behaviour in workers (Slessor et al., 1988). Two additional components, methyl *p*-hydroxybenzoate (HOB) and 4-hydroxy-3-methoxyphenylethanol (HVA), were discovered; they act synergistically with 9-ODA and 9-HDA to elicit retinue attraction, but do not work in isolation (Slessor et al., 1988; Slessor et al., 1990). The four-component blend also affects worker orientation during swarming and inhibits queen rearing (Winston et al., 1989).

The honey bee olfactory system displays a clear sexual dimorphism at both the peripheral and the central level. Apart from clear differences in the shape and size of worker and drone antennae (in the drone: shorter scapus but thicker and longer flagellum, with eleven instead of ten segments, as in the worker), the most impressive difference between the two sexes lies in the number of pore-plate sensilla: around 18 000 on a drone antenna, and only 2800 on a worker antenna (Esslen and Kaissling, 1976). This difference translates into differences in the number of olfactory sensory neurones (OSNs), which are around 330 000 in drones *vs* 46 000 in workers (Esslen and Kaissling, 1976). Electrophysiological studies have shown that this increased number of OSNs in the drone is also related to an increased probability of finding cells responding to 9-ODA than

in workers (Kaissling and Renner, 1968; Vareschi, 1971). Moreover, electroantennogram (EAG) recordings have shown a much higher response to 9-ODA or to a whole-queen extract in drones than in workers (Skirkeviciene and Skirkevicius, 1994; Vetter and Visher, 1997; Brockmann and Brückner, 1998). Vareschi (Vareschi, 1971) electrophysiologically identified a type of receptor cell (type I), which responded to 9-ODA and to a range of aliphatic acids. However, these cells were extremely sensitive to 9-ODA, with a detection threshold at least three orders of magnitude below that to other odours (Vareschi, 1971). At the central level, sexual dimorphism is present at the first olfactory centre, the antennal lobe (AL). In worker bees, the AL consists of ~160 identified functional units, the glomeruli, which are interconnected by approximately 4000 local, inhibitory interneurons (Fonta et al., 1993). OSNs project onto such glomeruli *via* the antennal nerve and processed olfactory information leaves the AL by approximately 800 projection neurons, toward higher-order brain centres, such as the mushroom bodies or the lateral protocerebrum (Abel et al., 2001). In drones, sensory tracts are thicker but project into a smaller number of glomeruli than in workers (Arnold et al., 1985). Most of them (~103) correspond to glomeruli of a similar size to those of workers (henceforth called 'ordinary' glomeruli). However, the most dramatic difference between the drone and the worker AL is the presence of four hypertrophied glomeruli in the drone, the macroglomeruli (Arnold et al., 1985). Based on their impressive size and their similarity to the macroglomerular complexes of males of several moth species, which are involved in the detection and processing of female pheromone components, it was proposed that the macroglomeruli of drone honeybees play a similar role and serve the detection and processing of queen pheromonal components (Arnold et al., 1985; Masson and Mustaparta, 1990). Besides pheromonal detection, the olfactory system of drones can also detect a wide range of different odorants, including floral odours and social pheromones, which it can learn to associate with a sugar reward in the classical conditioning procedure of the proboscis extension response (Vareschi, 1971; Becker et al., 2000). Until now, no study has addressed how pheromonal and plant odours are represented in the drone antennal lobe, or evaluated the role of the macroglomeruli in queen pheromone detection. The assumption that processing of queen pheromone components is restricted to the drone macroglomeruli therefore remains untested.

Optical imaging techniques provide a possible way to address this problem experimentally. These techniques allow measuring the activity of numerous neurons at the same time; in the worker honey bee, calcium imaging has been successfully applied to record neural activity both from the ALs (e.g. Joerges et al., 1997; Sachse and Galizia, 2002; Sandoz et al., 2003) and the mushroom bodies (e.g. Faber and Menzel, 2001; Szyszka et al., 2005). In the ALs, odours elicit combinatorial activity patterns across glomeruli (Joerges et al., 1997) and odour quality is represented by a specific distributed code, conserved between individuals (Galizia et al., 1999; Sachse et al., 1999). Activity patterns in the AL clearly correspond to a perceptual representation of odorants, as physiological similarity between activity patterns correlates with perceptual similarity as deduced from generalisation performances of bees conditioned to a wide spectrum of selected odours (Guerrieri et al., 2005). Using calcium imaging, I measured odour-evoked responses in the glomeruli of the drone AL to understand how information about queen pheromone components and other odours is represented in the drone brain. Odours belonging to three main classes of stimuli were presented: (i) queen pheromonal components, potentially used by drones for the recognition of queens during nuptial flights, (ii) social pheromonal components produced by workers and used for social cohesion in the colony, and (iii) floral odours, which are present in the food stores of the hive and/or brought back by foragers.

Materials and methods

Honey bee preparation

Apis mellifera L. drones were taken from an outdoor hive during the month of August. They were brought to the laboratory and fixed in a Plexiglas^{TM} recording chamber using low-temperature melting wax so that the head could not move. The preparation followed the method used for calcium imaging recordings at the level of the worker AL (Galizia et al., 1997; Sandoz et al., 2003), although some adaptations were required due to differences in the conformation of the drone head (in particular the big compound eyes and the short antenna scapi). The antennae were fixed to the front of the chamber using fine plastic threads and a two-component silicon glue (Kwik-Sil, World Precision Instruments). Small pieces of plastic foil (0.5 mm thick) were then waxed at an angle to the front, and vertically to the sides of the chamber, to create a small pool around the brain region. Thus the antennae remained in the air, whilst the brain region could be kept in saline solution. A window was then cut in the cuticle of the head, as a triangle between the eyes to the sides, and the antennae to the front. Because the antennal lobes are less accessible in the drone than in the worker bee, the cuticle constituting the articulations of the antennae (antennal sclerite) was removed very carefully. Glands and trachea were removed to reveal both antennal lobes, and the oesophagus was removed. The brain was then washed thoroughly with saline solution (in mmol l^{-1}: Nacl, 130; KCl, 6; $MgCl_2$, 4; $CaCl_2$, 5; sucrose, 160; glucose, 25; Hepes, 10; pH 6.7, 500 mOsmol; all chemicals from Sigma-Aldrich, Lyon, France). For staining, the saline solution was gently removed, and the brain was bathed with 50 μl of dye solution. The dye consisted of Calcium-Green-2AM (50 μg) dissolved with 50 μl Pluronic F-127 (20% in dimethylsufoxide, DMSO) in 800 μl Ringer (all from Molecular Probes, Eugene, OR, USA). The piece of head cuticle was then replaced onto the opening and the drone was left for 1 h on ice. After staining, the brain was thoroughly washed with saline.

Optical recordings of odour-evoked activity

In vivo calcium imaging recordings were carried out using

a T.I.L.L. photonics imaging system (Martinsried, Germany). Stained bees were placed under an epifluorescent microscope with a water-immersion objective (20×, NA 0.5), and the head region was immersed in saline solution. The preparation was slightly tipped to the front to offer a view of the antennal lobe surface with as few focus differences as possible between the different lobe regions. Images were taken using a 640×480 pixel 12-bit monochrome CCD-camera (T.I.L.L. Imago) cooled to –12°C. Each measurement consisted of 100 frames at a rate of 5 frames s^{-1} (interval between frames 200 ms), and the integration time was 15 ms. Odour stimuli were given at the 15th frame for 1 s. Pixel image size corresponded to ~5×5 μm after 4×4 binning on chip. Monochromatic excitation light at 475 nm was applied using a monochromator (T.I.L.L Polychrom IV). The filter set on the microscope was composed of a 505 nm dichroic filter and an LP 515 nm emission filter. Under the microscope, a constant air-stream, into which odour stimuli could be injected, was directed to the drone's antennae (distance 2 cm). During odour stimulation, a secondary airflow was diverted from the main airflow and passed through an interchangeable glass pipette containing the odour. Stimulations were controlled by the imaging system's computer. The floral odours used were 1-hexanol, 1-nonanol, limonene and +/–linalool (from Sigma-Aldrich) and clove and orange essential oils obtained from a drugstore (Berlin-Dahlem, Germany). Some social pheromonal components such as citral, geraniol (aggregation), isoamyl acetate and 2-heptanone (alarm) were only tested in a few animals (N=3). The queen pheromone components tested were: 9-keto-2 (E)-decenoic acid (9-ODA), 9-hydroxy-2 (E)-decenoic acid (9-HDA), 4-hydroxy-3-methoxyphenylethanol (HVA) and methyl *p*-hydroxybenzoate (HOB). Another component, 10-hydroxy-2 (E)-decenoic acid (10-HDA), which is present in high amounts in both workers and virgin queens (Plettner et al., 1997) was also included. Odour sources were prepared by applying 5 μl of substance (floral odours and social pheromones) or 5 μl of substance diluted in isopropanol (queen pheromone components, concentration of 5 μg μl^{-1}) onto a 1 cm^2 piece of filter paper inserted in a Pasteur pipette. When preparing the pheromone sources, the solvent was allowed to evaporate for 30 s before the pipette was closed. As control stimuli, pipettes containing a clean piece of filter paper (air control) or a filter paper with 5 μl of isopropanol (2prop; also evaporated) were used. An experimental run consisted of three fully randomised series of 10–13 odour presentations with 1–2 min inter-trial intervals.

Mapping activity onto glomeruli

During optical imaging, the glomerular structure of the antennal lobes is not visible and fluorescence is homogeneous over the whole AL surface. To reveal the glomerular AL structure after performing the calcium imaging recordings, standard techniques developed for worker bees were used (Galizia et al., 1999). Briefly, a mixture 125:1 (v/v) of a protease solution (from *Bacillus licheniformis* in propylene glycol; Sigma Aldrich) for digesting the brain sheath, and of the dye RH795 (dissolved in absolute ethanol) for staining cell membranes (Molecular Probes), was applied to the brain for 1 h. Afterwards, the brain was rinsed with saline solution and fluorescent photographs were taken at 5–10 different focal planes under 530–540 nm excitation light, using a filter set containing a 570 nm dichroic mirror and a LP 590 nm emission filter. One particularly large activity spot situated on the dorso-lateral side of the antennal lobe was clearly identified as the second macroglomerulus MG2, based on its location [(Arnold et al., 1985); see Fig. 1A] and on the direct comparison of imaging data and anatomical stainings carried out after imaging. Its direct medial neighbour, MG1, was recognised only on the basis of anatomical stainings, as no signals were recorded in this macroglomerulus (see Results). Concerning ordinary glomeruli, anatomical stainings after imaging showed limited success in revealing their layout and numbers. In a few cases in which the glomerular layout could be resolved, activity spots clearly corresponded to individual glomeruli (see Fig. 1). Later, additional stainings on drones not subjected to calcium imaging were performed, replacing RH795 by a 4% solution of Neutral Red in distilled water. These stainings gave much better results and allowed confirmation of the general layout of the drone AL (see Fig. 1A).

Signal calculation

Calcium-imaging data were analyzed using custom-made software written in IDL (Research Systems Inc., Boulder, CO, USA). Each recording to an odour stimulus corresponded to a 3-dimensional matrix with two spatial dimensions (x, y pixels of the area of interest) and a temporal dimension (100 frames). Three steps were carried out to calculate the signals: first, to reduce photon (shot) noise, the raw data were filtered in the two spatial and in the temporal dimensions using a median filter with a size of 3 pixels. Second, relative fluorescence changes (called $\Delta F/F$) were calculated as $(F–F_0)/F_0$, taking as reference background F_0 the average of three frames before any odour stimulation (here frames 5–7). Third, to correct for bleaching and possible irregularities of lamp illumination in the temporal dimension, a subtraction was made at each pixel of each frame, of the median value of all the pixels of that frame. Such a correction stabilizes the baseline of the recordings, without removing pertinent signals. Odour-evoked signals were the typical stereotyped biphasic signals usually obtained with bath application of Calcium Green, with first a fast fluorescence increase, followed by a slow fluorescence decrease below baseline (Fig. 1E); (Galizia et al., 1997; Stetter et al., 2001; Sandoz et al., 2003). The maximum signal was obtained 1.0–1.2 s after odour application and the minimum 8–10 s after odour application (Fig. 1E).

For visual observation of the signals in the different AL regions (Figs 1, 2 and insets in Fig. 3), activity maps are shown with the best possible spatial definition of odour-induced signals. Therefore, the full signal amplitude was used. Each pixel represented the mean of three frames after 1 s (i.e. from

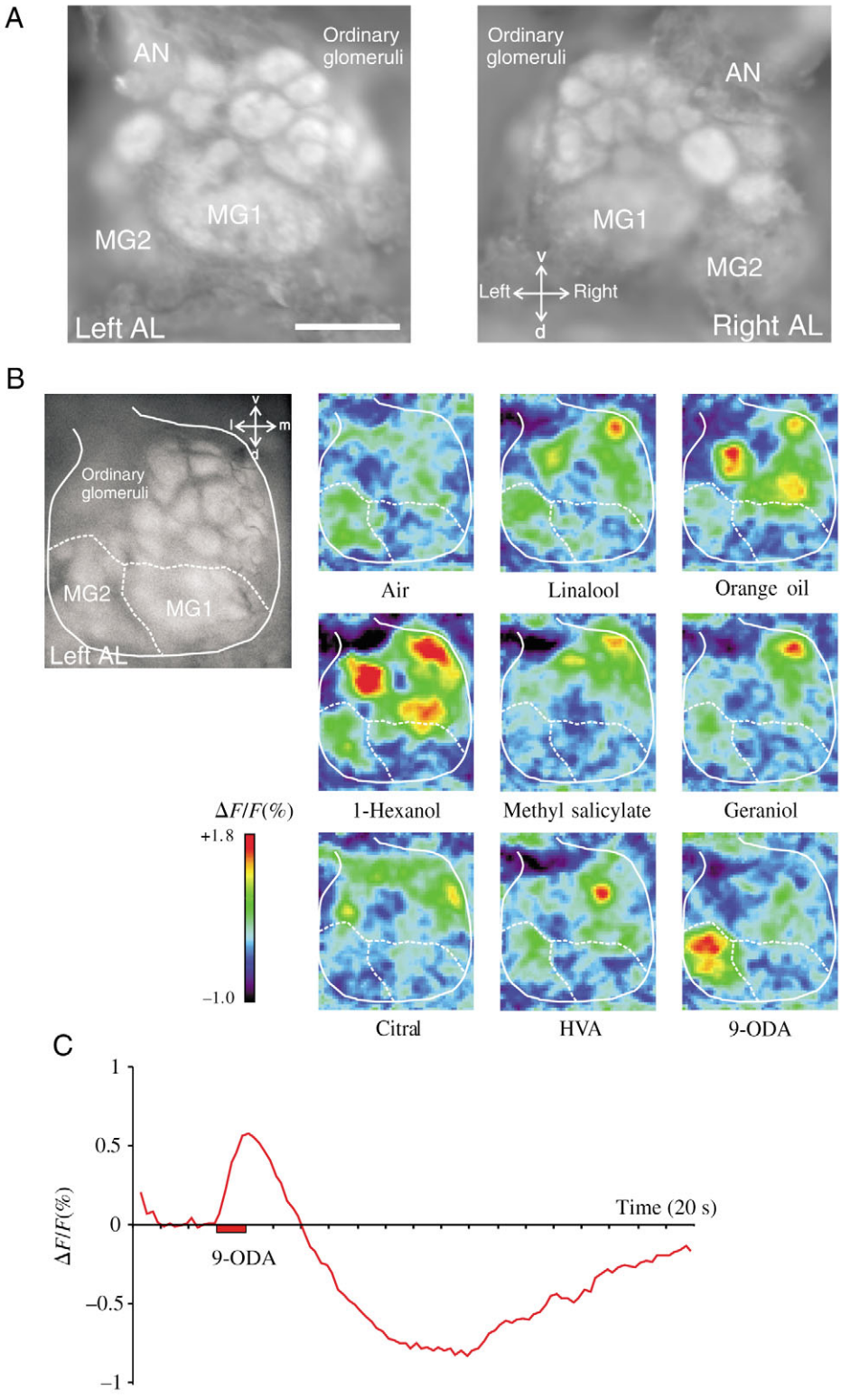

Fig. 1. Calcium signals in the drone antennal lobe. (A) Anatomical layout of the regions of the drone antennal lobe accessible to optical imaging experiments. An anatomical staining (Neutral Red) of the two antennal lobes of a drone, indicating a ventral region rich in ordinary glomeruli, and a dorsal region containing 2 macroglomeruli (MG1 and MG2). AN, antennal nerve; v, ventral; d, dorsal. Scale bar, 100 μm. (B) Calcium signals in a drone. Upper left: antennal lobe layout of the drone for which the calcium signals are presented. l, lateral; m, medial. Right: activity maps for odour-induced calcium signals in a drone antennal lobe. Relative fluorescence changes ($\Delta F/F\%$), taken between the maximum after 1 s and the minimum after 9 s (see C) are presented in a false-colour code, from dark blue to red for different floral odorants (linalool, 1-hexanol, methylsalicylate), a floral blend (orange oil), social pheromones (geraniol and citral) and queen pheromonal components (9-ODA, HVA). Different odours induce different activity patterns, either in the region of ordinary glomeruli or in MG2. (C) Typical time course of relative fluorescence changes ($\Delta F/F\%$) in the course of a recording. The presented signal was recorded in MG2 in response to the queen pheromonal component 9-ODA.

0.6 to 1.2 s) minus the mean of three frames after 9 s (i.e. from 8.6 to 9.2 s). Activity maps are presented in a false-colour code, from dark blue (no signal) to red (maximum signal).

For quantitative analysis of signal amplitudes (Figs 3 and 4), the analysis focused, as in previous work (Galizia et al., 1999; Sachse et al., 1999; Sandoz et al., 2003), on the fast (positive) signal component evoked by odour stimulation. There are several reasons for this choice. First, this calcium increase on odour stimulation can be ascribed to an intracellular calcium increase from the extracellular medium, directly related to

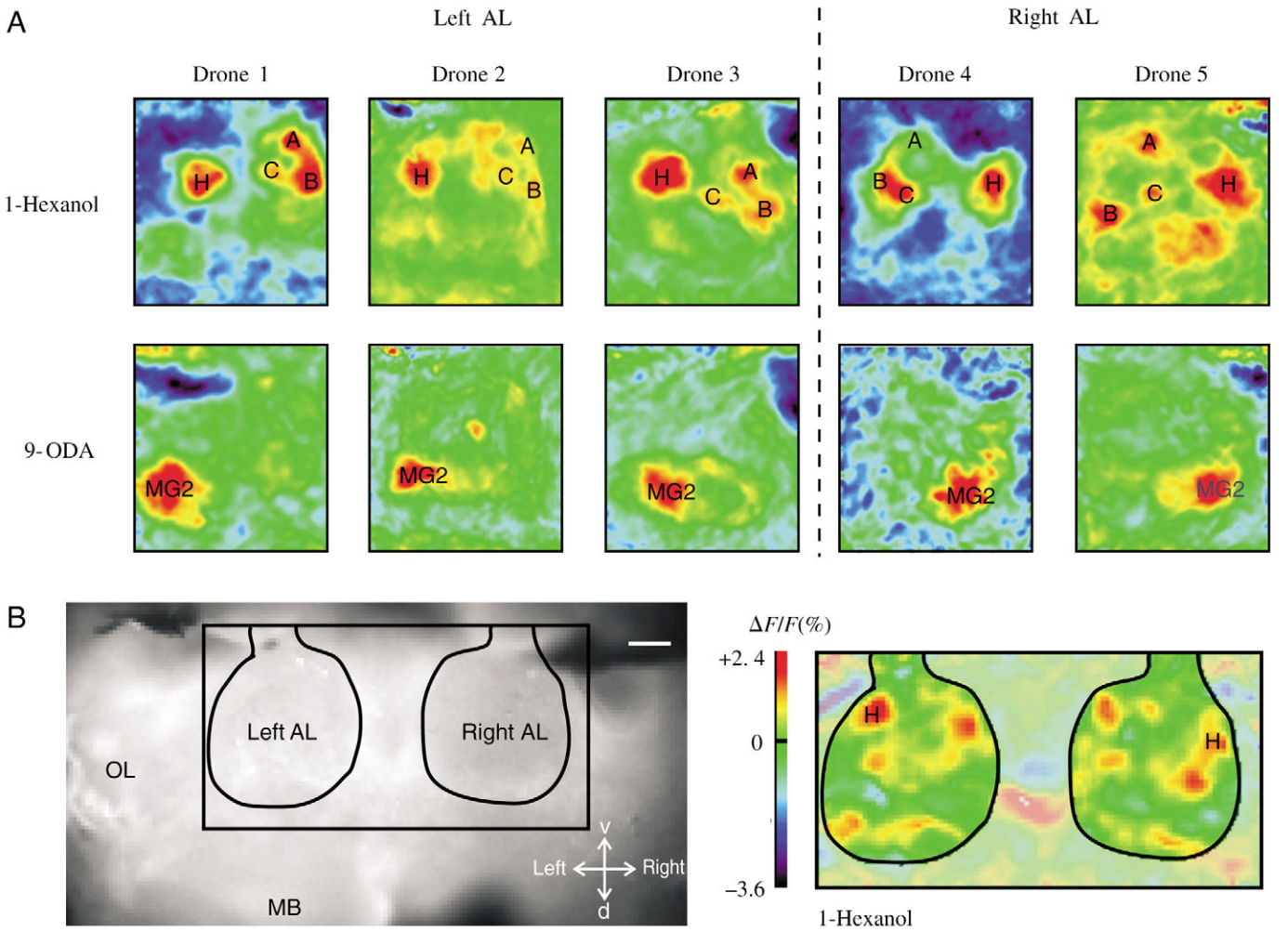

Fig. 2. Inter-individual conservation and bilateral symmetry of odour-induced signals in the drone antennal lobe. (A) Calcium signals obtained in five different drones (1–5), on three left and two right antennal lobes (AL) to the odours 1-hexanol and 9-ODA. Each activity map (calculated as in Fig. 1) is scaled to its own minimum and maximum. While 1-hexanol triggers in all five antennal lobes, a similar pattern of a few activated glomeruli [in particular a large egg-shaped glomerulus (H) on the ventro-lateral side], 9-ODA induces activity almost exclusively in the large dorso-lateral region corresponding to MG2. The arrangement of activated glomeruli is symmetrical in left and right antennal lobes. (B) Simultaneous bilateral optical imaging of the drone AL. On the left, a view of the brain showing the recording window and the localisation of the ALs. Scale bar, 100 μm. On the right, a recording to 1-hexanol showing symmetrical activity patterns in four glomeruli in each lobe. Note that glomerulus H can be identified in both lobes. OL, optic lobe; MB, mushroom bodies; v, ventral; d, dorsal.

neuronal activity (see also Galizia and Kimmerle, 2004). It reflects most probably pre-synaptic neuronal activity from OSNs (Galizia et al., 1998; Sachse and Galizia, 2003). Second, studies recording neuronal responses downstream along the olfactory pathway showed that these neurons [projection neurons and clawed Kenyon cells (Sachse and Galizia, 2002; Szyszka et al., 2005)] respond well within the first second after odour application. For each activity spot studied, the time course of relative fluorescence changes was calculated by averaging 25 pixels (5×5). The amplitude of odour-induced responses was calculated as the mean of 3 frames after odour onset (i.e. 0.6–1.2 s) minus the mean of 3 frames just before the odour stimulus (i.e. –0.8 to –0.2 s). This value was then used in all computations.

Measuring odour similarity in drones

One aim of this study was to measure the similarity between different odorants based on the signals obtained in the region of ordinary glomeruli. Because anatomical stainings did not allow all glomeruli present at the AL surface to be distinguished during imaging, the study was focussed on the activity spots (between N=10 and N=18) observed in each drone. As a measure of similarity between odours, the Euclidian distance between odour representations in a putative n-dimensional space in which the activity of each spot represents one dimension was calculated. The higher the calculated distance between odour representations, the less similar were the odour representations. For each odour pair, distances calculated in each individual were averaged and subjected to a correlation

analysis with previous data on honeybee workers (Galizia et al., 1999; Sachse et al., 1999; Sandoz et al., 2003). For calculating distances between odour representations based on imaging data (Galizia et al., 1999; Sachse et al., 1999), a method was used that gave good results in a previous report (Guerrieri et al., 2005): AL activation maps (as presented on http://neuro.uni-konstanz.de/) were thus transcribed into activation levels for each glomerulus from 0 to 3, according to the following signal scale: activity below 40%, 0; 40–60% activity, 1; 60–80% activity, 2; >80% activity, 3. As a second comparison between odour similarity in drones and workers, data from a previous study, using naïve bees only (Sandoz et al., 2003), were used. As this study carrying out bilateral optical imaging of both ALs showed that odour-induced activity of naïve bees is symmetrical, the signals from right and left antennal lobes were averaged within each individual. The signal amplitudes recorded in the 24 AL glomeruli recognized in Sandoz et al. (Sandoz et al., 2003) were used to calculate Euclidian distances between odour representations as was done with drone data. The significance of all linear correlations was assessed by calculating Pearson's *r*, and using Student's *t*-test.

Results

Anatomical layout of the drone antennal lobe

Fig. 1A presents anatomical stainings of the frontal part of the drone antennal lobe accessible to optical imaging. The AL can be roughly divided into two halves. The ventral half carries only ordinary glomeruli, among which a few are particularly conspicuous due to their particular shape or size (Fig. 1A). The dorsal half shows two large areas that correspond to the first two (out of four) macroglomeruli: MG1 is located dorso-medially, while MG2 is situated on the dorso-lateral side. The anatomical layout of the drone AL is clearly symmetrical between brain hemispheres. The antennal nerve appears on the ventro-lateral side of each AL.

Odours evoke calcium signals in the glomeruli of the drone antennal lobe

Thirty four drones were prepared for optical imaging experiments, 12 of which allowed recording of calcium signals in response to odours. Fig. 1B,C present a typical example of odour-evoked calcium signals in the drone antennal lobe. Calcium signals were always observed in topical foci, which were different for different odours (Fig. 1B). The location of the activated foci corresponded to two distinct anatomical regions: the ventral region of ordinary glomeruli, and the dorso-lateral region of the lobe corresponding to MG2. No odour-induced responses were observed in the dorso-medial region corresponding to MG1. Although anatomical after-stainings usually gave limited success in revealing the layout of ordinary glomeruli, in some instances it could be clearly seen that the activity foci in the dorsal region originated in individual ordinary glomeruli (Fig. 1B). Control odours (air or 2-propanol) usually induced no or very low signals. In all imaged drones, the calcium signals showed typical biphasic time courses like the ones observed with the same staining method in workers [bath-applied Calcium Green 2-AM (Galizia et al., 1997)]. This time course was similar in all glomerular types (ordinary glomeruli or macroglomerulus), and was the same for pheromonal and floral odours. After odour application (Fig. 1C, example with 9-ODA), fluorescence increased topically, reaching a maximum after 1.0–1.2 s (fast positive component), before decreasing to a minimum, about 8–10 s after odour application (slow negative component). Apart from a small bleaching effect in some recordings, the signal increased again to near-baseline within 20 s. Because other studies have shown that neuronal responses downstream along the olfactory pathway respond well within the first second after odour application [projection neurones and clawed Kenyon cells (Sachse and Galizia, 2002; Szyszka et al., 2005)], further analysis concentrated on the fast positive component.

Odour-induced calcium signals were reproducible within an individual as well as between individuals (Fig. 2A) and were also symmetrical between brain hemispheres. Fig. 2A presents the responses observed in five different individuals (three left and two right antennal lobes) to 1-hexanol and to the pheromone component 9-ODA. Clearly, 1-hexanol induced activity in one large ordinary glomerulus (H in the Fig. 2A) on the ventro-lateral side of the antennal lobe, and in two to three smaller glomeruli (A, B and C in Fig. 2A) on the ventro-medial side. This arrangement was found symmetrically in left and right antennal lobes (Fig. 2A). Similarly, response to 9-ODA was in all drones found in the same region, corresponding to MG2. When optical recordings were carried out simultaneously on the two antennal lobes (Sandoz et al., 2003), a symmetrical arrangement of active glomeruli was clearly found (Fig. 2B).

Queen pheromonal components activate both ordinary glomeruli and one macroglomerulus

The drones were presented with five queen pheromonal components: 9-ODA, 9-HDA, 10-HDA, HVA and HOB. Responses to these components were of three types.

Fig. 3. Response spectra recorded in identified glomeruli of the drone antennal lobe. (A) Amplitude of calcium responses ($\Delta F/F\%$, positive signal 1 s after odour onset) to queen pheromone components and control stimuli recorded in the two macroglomeruli (boxed; mean ± s.e.m., N=11 drones). Only the major component 9-ODA induces clear calcium signals in MG2. MG1 does not respond. ***P<0.001 for all pair-wise Scheffé comparisons. (B) Comparison of responses in three different regions (F1–3; boxed) of MG2 in a subset of the drones (N=5), to the queen pheromone components, the control stimuli and all floral odours in common for these drones. No difference is observed between the response spectra of the three foci: all respond specifically to 9-ODA. (HEX, 1-hexanol; LIO, linalool; ORA, orange oil). (C) Responses of two ordinary glomeruli (boxed) responding to the pheromone components HOB (ventral glomerulus) and HVA (central glomerulus), respectively, in the five drones in which these glomeruli were clearly seen. Responses to the queen pheromone components, the control stimuli and all floral odours in common for these drones are presented (NON, 1-nonanol; LIM, limonene; CLV, clove oil).

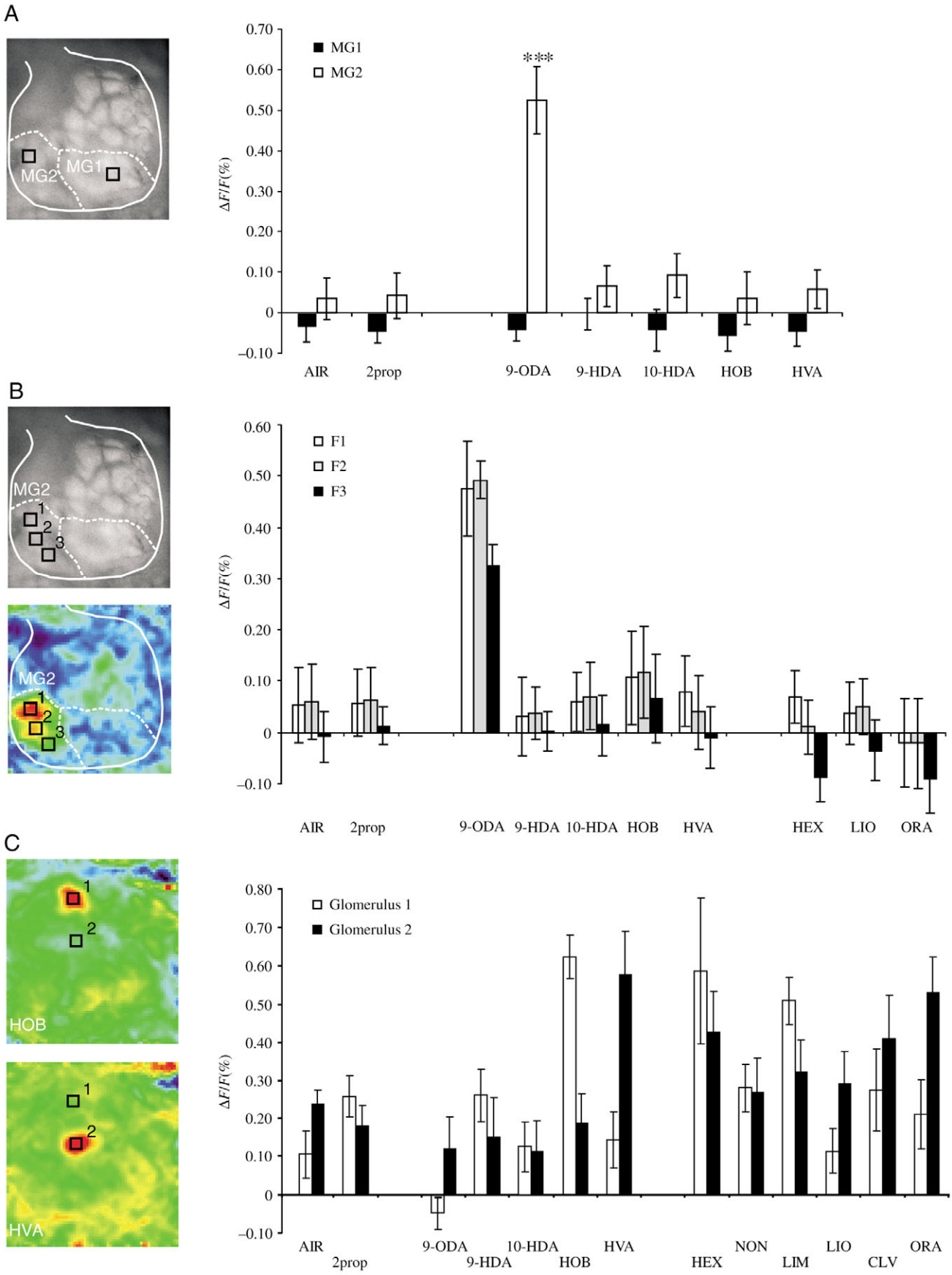

Fig. 3. For legend see previous page.

First, as shown above (Fig. 2A), the major component of the queen pheromone 9-ODA consistently induced calcium signals in the dorso-lateral region corresponding to MG2. This response was very clear and appeared in all individuals that showed calcium signals (N=12). Moreover, it was very specific: 9-ODA did not induce signals in other AL regions, and no other odour tested activated MG2 efficiently. In some cases, other odours could be seen to induce very low responses in MG2, but these could not be distinguished from air or 2-propanol controls. To document the specificity of MG2 responses to 9-ODA, Fig. 3A shows the responses recorded to the five queen pheromonal components and the two control stimuli (air control, and 2-propanol solvent) (N=11 drones, overall 32 stimulations with each odour). In MG2, the only response above baseline was to 9-ODA (0.52±0.08%) as confirmed by a two-way stimulus×macroglomerulus ANOVA (both repeated factors): both stimulus and macroglomerulus factors were significant ($F_{6,60}$=14.4, P<0.001; $F_{1,10}$=11.5, P<0.007 respectively), and the only significant heterogeneity detected by *post-hoc* Scheffé contrasts was between 9-ODA and each of the other stimuli (P<0.001 in all cases). In some recordings, signals in MG2 seemed spatially heterogeneous, with some areas showing higher activity than others (see, for instance, the response to 9-ODA in Fig. 1B). Based on this observation, and because anatomical findings suggested that the drone macroglomeruli may contain different subunits, and therefore correspond functionally to a macroglomerular complex (Arnold et al., 1985), it was important to check whether different zones of the macroglomerulus may respond differentially to the presented odours. Three different foci were placed in the five best drone recordings, which allowed seeing the borders of MG2. The first focus (F1) was the point of activity to 9-ODA, which was at the most frontal-lateral part of MG2. The other two foci (F2, F3) were regularly placed along the length of MG2 in a medio-lateral axis. Fig. 3B presents the amplitude of responses of these three foci to the range of odours tested in these drones (eight odours and two control stimuli). In all three parts of the macroglomerulus, significant responses were only recorded for 9-ODA, and no qualitative difference in odour responses appeared among the three foci. A two-way ANOVA stimulus×focus (repeated measures) indicated that both factors were significant ($F_{9,36}$=6.63, P<0.001, and $F_{2,8}$=6.6, P<0.05), but most importantly that no interaction was found between the factors ($F_{18,72}$=0.71, NS). Thus the significant difference between foci is attributable to intensity differences (the third focus showing less response to 9-ODA than the other two) and not to different odour response spectra. Thus, all parts of MG2 accessible to optical imaging responded specifically to 9-ODA and appeared to correspond to a single functional unit.

In contrast to 9-ODA, the queen pheromone components HOB and HVA induced activity mostly in two ordinary glomeruli in the centre of the frontal region (N=7/12 drones): the HOB glomerulus was usually a more ventral neighbour of the HVA glomerulus. In contrast to 9-ODA in MG2, the HOB and HVA glomeruli commonly showed responses to floral odorants. Fig. 3C presents response profiles of these two glomeruli in five individuals in which the two glomeruli were identified. While glomerulus 1 responded to HOB, glomerulus 2 responded to HVA. However, glomerulus 1 responded clearly to 1-hexanol and to limonene, and glomerulus 2 mostly responded to 1-hexanol and to the clove oil and orange oil blends. Thus, these glomeruli did not respond specifically to HOB and HVA. Lastly, 9-HDA and 10-HDA induced only very low and diffuse signals in some ordinary glomeruli and/or in MG2. However, these signals were inconsistent and could not be differentiated from control stimuli. Therefore they were not quantified.

A combinatorial response table in the drone antennal lobe

As indicated above, floral odours and mixtures presented to the drones induced focal calcium responses on the ventro-medial side of the antennal lobe (N=12 drones), a region rich in ordinary glomeruli. Different odours activated specific sets of ordinary glomeruli (from one to six) in a combinatorial manner. Different odours could also activate the same glomerulus, as shown in Fig. 1B, where most odours activated the upper-right glomerulus, while only 1-hexanol and orange oil activated the glomerulus on the right, above MG1. Social pheromonal components were only tested in a few individuals. Geraniol and citral induced signals only in ordinary glomeruli while isoamyl acetate and 2-heptanone did not give any measurable signals (N=2–3 individuals). The combinatorial responses obtained to floral odours in ordinary glomeruli are represented as the responses of activity foci (size >25 μm i.e. 5 pixels) that responded to any of the odour stimulations. An example of such a combinatorial activity table is given in Fig. 4A (mean of three stimulations with each odour in one drone). Most odour-induced activity is visible in ordinary glomeruli (numbered 1–10; see Fig. 4B for localisation), which responded in a combinatorial manner to the six floral odours. The only pheromone components that induced responses in ordinary glomeruli were HOB and HVA. MG2 responded to 9-ODA and not to other odours. Responses to the diluted queen pheromone probes usually had lower amplitudes than responses to the pure floral odours, which explains how pheromone responses only reach the green category (40–60% of maximum response) in Fig. 4A.

The search for similar glomeruli in different individuals was difficult due to the fact that no glomerular atlas of the drone antennal lobe is yet available. However, five ordinary glomeruli were tentatively described in the five best drones, according to (1) their relative position in the antennal lobe; (2) their size; (3) their odour response profiles. These glomeruli are presented in Fig. 4B on the same drone as in Fig. 4A: the most prominent ordinary glomerulus was localised on the ventro-lateral side, was egg-shaped and responded strongly to 1-hexanol and to orange oil (corresponds to glomerulus H in Fig. 2A). Two other glomeruli were the HOB and HVA glomeruli described above, placed ventrally and in the centre of the AL. Lastly, two glomeruli on the medial side responded strongly to limonene (and in some drones to linalool) in the case of the more ventral one, and to 1-hexanol in the case of the more dorsal one.

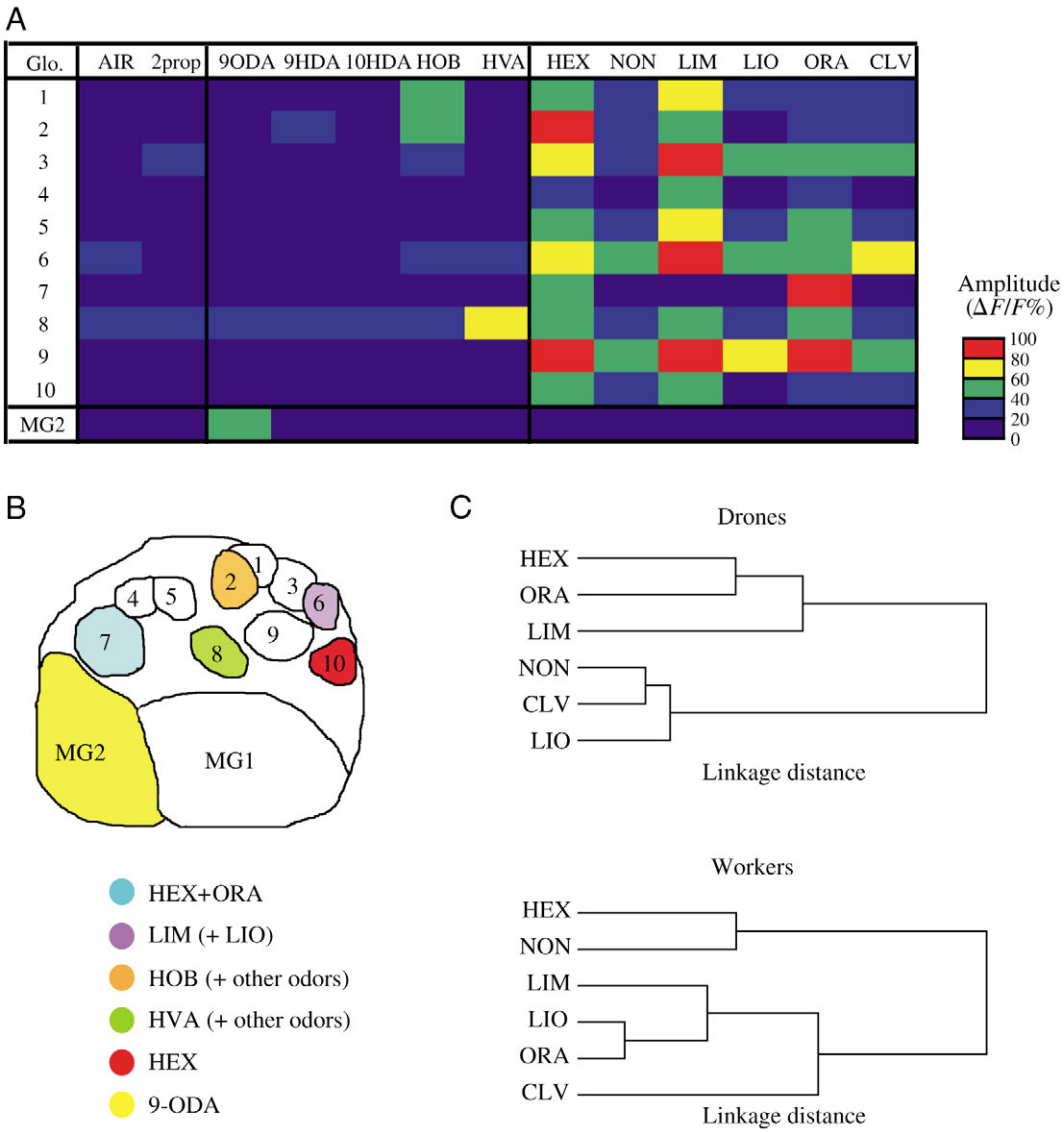

Fig. 4. Combinatorial activity patterns to floral odours in the drone antennal lobe and comparison of similarity relationships between drones and workers. (A) Combinatorial response table in a drone. Responses to queen pheromone components, control stimuli and floral odours in ten ordinary glomeruli (Glo.1–10) are colour-coded according to the relative amplitude of the response in this individual. Floral odours induce activity in a combination of ordinary glomeruli. (B) Schematic anatomical layout of the antennal lobe for the same drone as in A. The glomeruli that could be recognised in different individuals (N=5) from their response spectrum, relative position, size and shape are presented in different colours, with their main activating odours. (C) Cluster analyses showing similarity relationships between odours in drones and in workers (using the Euclidian distance between odours in a putative n-dimensional space corresponding to the n measured glomeruli in each individual). Top: drones (N=5). Bottom: workers [datasets of (Galizia et al., 1999; Sachse et al., 1999)]. Similarity relationships among odours are clearly different in the two datasets. For abbreviations, see legend to Fig. 3.

Similarity among odours measured in drone and worker antennal lobes

Even though individual glomeruli can be tentatively recognised in different drones, building a physiological response atlas, as was successfully carried out for the worker bee (Sachse et al., 1999) is not possible. Nevertheless, the similarity in calcium activity patterns elicited by different odorants can be evaluated within each individual. Such a measure is independent of the identity of each particular glomerulus, as long as the same glomerular ensemble is considered in the different individuals, which is the case in this study. Based on activity in ordinary glomeruli, similarity relationships among odours were compared in drones and in workers [datasets (Galizia et al., 1999; Sachse et al., 1999)]. Cluster analyses based on glomerular responses in both castes showed clearly different arrangements (Fig. 4C). In workers, three main clusters appeared, which grouped (1) two alcohols (1-hexanol and 1-nonanol), (2) two terpenes (linalool and limonene) and the orange oil mixture, and (3) the clove oil mixture, respectively. In contrast, in drones, two clusters

appeared, which grouped (1) 1-hexanol, limonene and orange, and (2) nonanol, linalool and clove oil, respectively. Correlation analyses representing Euclidian distances between odour representations in drones in function of the same measure in workers did not show any hint of correlation (data not shown, r=0.08, NS, 15 odour pairs). A similar analysis performed with the odours common in this and a previous study [all odours except linalool (Sandoz et al., 2003)] also did not show any correlation between drone and worker odour-similarity relationships (data not shown, r=0.08 also, NS, 10 odour pairs).

Discussion

This study presents the first successful *in vivo* optical imaging recordings of the antennal lobe of honeybee drones. It shows that: (i) the macroglomerulus MG2 responds specifically to the main queen pheromone component 9-ODA. (ii) Two other queen pheromone components, HOB and HVA, induced consistent signals in ordinary glomeruli. (iii) Different floral odours induce calcium signals in specific subsets of ordinary glomeruli. However, (iv) similarity relationships among odours measured in drones did not correlate with similar measures made on workers in previous studies.

Among the identified queen pheromone components (Slessor et al., 1988), three gave clear signals in the drone antennal lobe: 9-ODA, HOB and HVA. By contrast, 9-HDA and the virgin-queen and worker component 10-HDA showed no consistent signals in the glomeruli that could be imaged. The specificity of MG2 responses to 9-ODA confirms the hypothesis that the very conspicuous drone macroglomeruli would be involved specifically in pheromone detection and processing (Arnold et al., 1985; Masson and Mustaparta, 1990). The fact that MG2 is the most voluminous macroglomerulus of the drone AL (Arnold et al., 1985; Brockmann, 1999; Brockmann and Brückner, 2001) fits well with previous electrophysiological studies, which showed that an important part of the drone peripheral olfactory system is dedicated to the detection of 9-ODA (Kaissling and Renner, 1968; Vareschi 1971; Skirkeviciene and Skirkevicius, 1994; Brockmann and Brückner, 1998; Vetter and Visher, 1997). However, a previous anatomical study suggested that MG2 is not originally a single hypertrophied glomerulus, but rather the result of the fusion of several glomeruli (Arnold et al., 1985). In some recordings, signals in MG2 were not spatially homogenous, but showed what appeared to be small activity regions along the macroglomerulus' long axis. However, no indication was found of any heterogeneity in the responses of MG2 along this axis. Rather, the different regions responded to 9-ODA but not to other stimuli. Therefore, similar to moths, in which a clear odotopic projection of pheromone-specific OSNs to the macroglomerular complex is found, the results of the present study suggest that most (if not all) of the OSNs tuned to 9-ODA project to MG2.

One intriguing result of the present study is the absence of odour-induced signals in MG1, the second most voluminous macroglomerulus of the drone AL. It is unlikely that this observation is due to specific loading problems of the AM-dye in MG1, since during calcium imaging, fluorescence was found to be homogeneous over the whole AL, including MG1. Since the odours were tested at relatively high concentrations, concentration effects should not account for this result. A more likely explanation is that the odorant(s) detected by neurons projecting to MG1 were not among the panel of tested odours. An interesting hypothesis is that MG1 would process information about still unknown odorants involved in mating. Since the initial description of a queen mandibular extract reproducing the retinue behaviour of worker bees, which led to the use of 9-ODA, 9-HDA, HVA and HOB (Slessor et al., 1988), new components have been isolated that also have an effect on worker retinue: methyl oleate, coniferyl alcohol, hexadecane-1ol and linolenic acid. These components, which do not work isolated on retinue, but synergistically with the synthetic queen mandibular pheromone (Keeling et al., 2003), should be tested in imaging conditions. However, it must be emphasised that the search for queen pheromonal components has mainly focussed on creating blends able to accurately reproduce workers' – but not drones' – behaviour (Slessor et al., 1988; Keeling et al., 2003). It is generally acknowledged that drones are drawn to 9-ODA from long distances (Gary, 1962) and that 9-ODA alone does not always reproduce the effect of a complete queen extract in attraction bioassays (Pain and Ruttner, 1963). Thus, while 9-ODA is clearly the main attractant, the question of co-attractants is still unresolved. Interestingly, apart from their important role in queen fighting (Pflugfelder and Königer, 2003), it seems that once a drone is in the queen's vicinity the initiation of mating is triggered, or at least enhanced, by olfactory substances from the queen's tergite glands (Renner and Baumann, 1964; Renner and Vierling, 1977). A hypothesized function for MG1 could be the detection of such a releaser pheromone. All in all, future work should therefore test queen gland extracts under imaging conditions in order to find possible new candidate odours that may be detected and processed by MG1.

Responses to HVA and HOB occurred mainly in two ordinary glomeruli that responded to several floral odorants (Fig. 3C). This observation suggests that the responses obtained to HVA and HOB correspond to their detection by the general olfactory system and not to a pheromonal subsystem. The fact that responses to queen pheromone components were not circumscribed to the macroglomeruli and could be found in ordinary glomeruli would underline functional differences rather than similarities between the macroglomerular complex of male moths and that of drone honeybees. However these differences may be only apparent. In fact, virgin queens produce no HVA and very little HOB in comparison to mated queens (Plettner et al., 1997) such that these compounds could be only important for the induction of workers' retinue behaviour by mated queens, and not for drone attraction by virgin queens. In a similar way, 9-HDA and 10-HDA failed to induce consistent signals in the present recordings. Overall, so far, one study found attraction to 9-HDA (Butler and Fairey,

1964) but two subsequent studies failed to reproduce this finding (Blum et al., 1971; Boch et al., 1975). It could thus be that, as for HVA and HOB, these compounds play a crucial role in queen retinue but are not important in the mating process. Caution should, however, be exercised, because two additional macroglomeruli, which were not accessible in this imaging study, are present in the drone AL (Arnold et al., 1985).

Calcium signals to a range of floral odorants in ordinary glomeruli of the drone AL were similar to those usually observed in worker bees (Joerges et al., 1997; Galizia et al., 1997; 1999; Sachse et al., 1999): different odours induced signals in a specific subset of glomeruli. Although comparison between individual drones was made difficult by the fact that anatomical stainings did not give clear glomerular boundaries within ordinary glomeruli of most imaged drones, obvious similarities between individuals appeared. This suggests that the signals recorded in the anterior AL region represent part of a conserved neural across-fibre pattern through which plant odours are encoded in the drone brain. However, odour similarity relationships were clearly different from those described in workers in previous studies. This observation should be taken with caution. Because the macroglomeruli represent about half of the anterior surface of the drone AL, the ordinary glomeruli accessible to imaging are relatively few, about 20 out of 103 (Arnold et al., 1985). This proportion is similar to the ~30 glomeruli out of 160 routinely imaged in the worker (Galizia et al., 1999). Therefore this finding is probably due to the fact that the glomeruli imaged in the two castes are not homologous, i.e. that they do not correspond to the projection of OSNs expressing the same subsets of olfactory receptors. In the present study, neither anatomical observation of glomerulus position, size or shape, nor the respective arrangements of glomeruli activated by the different odours, showed any similarity with the workers. Future work will have to establish to what extent the functional arrangement of glomeruli is conserved between drones and workers.

List of abbreviations

10-HDA	10-hydroxy-2 (E)-decenoic acid
2prop	isopropanol
9-HDA	9-hydroxy-2 (E)-decenoic acid
9-ODA	9-keto-2 (E)-decenoic acid
AL	antennal lobe
CLV	clove oil
DMSO	dimethyl sulphoxide
EAG	electroantennogram
HEX	1-hexanol
HOB	methyl *p*-hydroxybenzoate
HVA	4-hydroxy-3-methoxyphenylethanol
LIO	+/–linalool
LIM	limonene
MG	macroglomerulus
NON	1-nonanol
ORA	orange oil
OSN	olfactory sensory neuron

I would like to warmly thank Prof. R. Menzel for his support and for particularly insightful discussions, Dr A. Brockmann for supplying the pheromonal compounds, and Dr D. Brückner and Prof. C. G. Galizia for helpful discussions while initiating this project. Thanks to Matthias Ditzen for recommending the use of Neutral Red for anatomical stainings. Thanks go to Prof. M. Giurfa, Prof. R. Menzel, Dr N. Deisig and two anonymous referees for helpful comments on the manuscript. I thank Mary Wurm for polishing the English. This work was funded by the Alexander von Humboldt Foundation and the French Centre National de la Recherche Scientifique (CNRS). Some of the experiments reported here were carried out at the Neurobiology Unit of the Freie Universität Berlin.

References

Abel, R., Rybak, J. and Menzel, R. (2001). Structure and response patterns of olfactory interneurons in the honeybee, *Apis mellifera*. *J. Comp. Neurol.* **437**, 363-383.

Arnold, G., Masson, C. and Budharugsa, S. (1985). Comparative study of the antennal lobes and their afferent pathway in the worker bee and the drone (*Apis mellifera*). *Cell Tissue Res.* **242**, 593-605.

Becker, M. M., Brückner, D. and Crewe, R. (2000). Behavioural response of drone honey bees, *Apis mellifera carnica* and *Apis mellifera scutellata*, to worker-produced pheromone components. *J. Apic. Res.* **39**, 149-152.

Blum, M. S., Boch, R., Doolittle, E., Tribble, M. T. and Traynham, J. G. (1971). Honey bee sex attractant: conformational analysis, structural specificity, and lack of masking activity of congeners. *J. Insect Physiol.* **17**, 349-364.

Boch, R., Shearer, D. A. and Young, J. C. (1975). Honeybee pheromones: field tests of natural and artificial queen substance. *J. Chem. Ecol.* **1**, 133-148.

Brockmann, A. (1999). Studies on the olfactory system of the honeybee drone, *Apis mellifera*. PhD thesis, University of Bremen, Germany.

Brockmann, A. and Brückner, D. (1998). The EAG response spectra of workers and drones to queen honeybee mandibular gland components: the evolution of a social signal. *Naturwissenschaften* **85**, 283-285.

Brockmann, A. and Brückner, D. (2001). Structural differences in the drone olfactory system of two phylogenetically distant *Apis* species, *A. florea* and *A. mellifera*. *Naturwissenschaften* **88**, 78-81.

Butler, C. G. and Fairey, E. M. (1964). Pheromones of the honeybee: biological studies of the mandibular gland secretion of the queen. *J. Apic. Res.* **3**, 65-76.

Esslen, J. and Kaissling, K. E. (1976). Zahl und verteilung antennaler sensillen bei der honigbiene (*Apis mellifera L.*). *Zoomorphologie* **83**, 227-251.

Faber, T. and Menzel, R. (2001). Visualizing a mushroom body response to a conditioned odor in honeybees. *Naturwissenschaften* **88**, 472-476.

Fonta, C., Sun, X. J. and Masson, C. (1993). Morphology and spatial distribution of bee antennal lobe interneurones responsive to odours. *Chem. Senses* **18**, 101-119.

Free, J. B. (1987). *Pheromones of Social Bees*. London: Chapman & Hall.

Galizia, C. G. and Kimmerle, B. (2004). Physiological and morphological characterization of honeybee olfactory neurons combining electrophysiology, calcium imaging and confocal microscopy. *J. Comp. Physiol. A* **190**, 21-38.

Galizia, C. G., Joerges, J., Kütnner, A., Faber, T. and Menzel, R. (1997). A semi-in-vivo preparation for optical recording of the insect brain. *J. Neurosci. Methods.* **76**, 61-69.

Galizia, C. G., Nägler, K., Hölldobler, B. and Menzel, R. (1998). Odour coding is bilaterally symmetrical in the antennal lobes of the honeybees (*Apis mellifera*). *Eur. J. Neurosci.* **10**, 2964-2974.

Galizia, C. G., Sachse, S., Rappert, A. and Menzel, R. (1999). The glomerular code for odor representation is species specific in the honeybee *Apis mellifera*. *Nat. Neurosci.* **2**, 473-478.

Gary, N. E. (1962). Chemical mating attractants in the queen honeybee. *Science* **136**, 1479-1480.

Guerrieri, F., Schubert, M., Sandoz, J. C. and Giurfa, M. (2005). Perceptual and neural olfactory similarity in honeybees. *PLoS Biol*. **3**, e60.

Joerges, J., Küttner, A., Galizia, C. G. and Menzel, R. (1997). Representations of odours and odour mixtures visualized in the honeybee brain. *Nature* **387**, 285-288.

Kaissling, K. E. and Renner, M. (1968). Antennale rezeptoren für queen substance und sterzelduft bei der honigbiene. *Z. Vergl. Physiol.* **59**, 357-361.

Keeling, C. I., Slessor, K. N., Higo, H. A. and Winston, M. L. (2003). New components of the honey bee (*Apis mellifera* L.) queen retinue pheromone. *Proc. Natl. Acad. Sci. USA* **100**, 4486-4491.

Masson, C. and Mustaparta, H. (1990). Chemical information processing in the olfactory system of insects. *Physiol. Rev.* **70**, 199-245.

Pain, J. and Ruttner, F. (1963). Les extraits de glandes mandibulaires des reines d'abeilles attirent les mâles lors du vol nuptial. *C. R. Acad. Sci. Paris* **256**, 512.

Pflugfelder, J. and Königer, N. (2003). Fight between virgin queens (*Apis mellifera*) is initiated by contact to the dorsal abdominal surface. *Apidologie* **34**, 249-256.

Plettner, E., Otis, G. W., Wimalaratne, P. D. C., Winston, M. L., Slessor, K. N., Pankiw, T. and Punchihewa, P. W. K. (1997). Species- and caste-determined mandibular gland signals in honeybees (*Apis*). *J. Chem. Ecol.* **23**, 363-377.

Renner, M. and Baumann, M. (1964). Über komplexe von subepidermalen drüsenzellen (Duftdrüsen) der bienenkönigin. *Naturwissenschaften* **51**, 68-69.

Renner, M. and Vierling, G. (1977). Die rolle des taschendrüsenpheromons beim hochzeitsflug der bienenkönigin. *Behav. Ecol. Sociobiol.* **2**, 329-338.

Sachse, S. and Galizia, C. G. (2002). The role of inhibition for temporal and spatial odor representation in olfactory output neurons: a calcium imaging study. *J. Neurophysiol.* **87**, 1106-1117.

Sachse, S. and Galizia, C. G. (2003). The coding of odour-intensity in the honeybee antennal lobe: local computation optimizes odour representation. *Eur. J. Neurosci.* **18**, 2119-2132.

Sachse, S., Rappert, A. and Galizia, C. G. (1999). The spatial representation of chemical structures in the AL of honeybees: steps towards the olfactory code. *Eur. J. Neurosci.* **11**, 3970-3982.

Sandoz, J. C., Galizia, C. G. and Menzel, R. (2003). Side-specific olfactory conditioning leads to more specific odor representation between sides but not within sides in the honeybee antennal lobes. *Neuroscience* **120**, 1137-1148.

Skirkeviciene, Z. and Skirkevicius, A. (1994). Worker bee and drone (*Apis mellifera* L.) behavior and functional reorganization of their olfactory receptors. *Pheromones* **4**, 83-92.

Slessor, K. N., Kaminski, L. A., King, G. G., Borden, J. H. and Winston, M. L. (1988). Semiochemical basis of the retinue response to queen honey bees. *Nature* **332**, 354-356.

Slessor, K. N., Kaminski, L. A., King, G. G. and Winston, M. L. (1990). Semiochemicals of the honeybee queen mandibular glands. *J. Chem. Ecol.* **16**, 851-860.

Stetter, M., Greve, H., Galizia, C. G. and Obermayer, K. (2001). Analysis of calcium imaging signals from the honeybee brain by nonlinear models. *Neuroimage* **13**, 119-128.

Szyszka, P., Ditzen, M., Galkin, A., Galizia, C. G. and Menzel, R. (2005). Sparsening and temporal sharpening of olfactory representations in the honeybee mushroom bodies. *J. Neurophysiol.* **94**, 3304-3313.

Vareschi, E. (1971). Duftunterscheidung bei der honigbiene–einzelzell-ableitungen und verhaltensreaktionen. *Z. Vergl. Physiol.* **75**, 143-173.

Vetter, R. S. and Visscher, P. K. (1997). Influence of age on antennal response of male honey bees, *Apis mellifera,* to queen mandibular pheromone and alarm pheromone component. *J. Chem. Ecol.* **23**, 1867-1880.

Winston, M. L. (1987). *The Biology of the Honey Bee*. Cambridge, MA: Harvard University Press.

Winston, M. L., Slessor, K. N., Willis, L. G., Naumann, K., Higo, H. A., Wyborn, M. H. and Kaminski, L. A. (1989). The influence of queen mandibular pheromone on worker attraction to swarm clusters and inhibition of queen rearing in the honeybee (*Apis mellifera* L.). *Insectes Soc.* **36**, 15-27.